ChemComm

COMMUNICATION

View Article Online
View Journal

Cite this: DOI: 10.1039/d6cc00925e

Received 11th February 2026,
Accepted 29th April 2026

DOI: 10.1039/d6cc00925e

rsc.li/chemcomm

Lanthanide tweezer complexes for luminescence detection of aromatic pollutants in water

Peter B. Glover,[a] Lauren Senkiw-Smith,[a] Linette L. Ruston,[a] Benson M. Kariuki[b] and Zoe Pikramenou *[a]

Red and green luminescence is sensitised by aromatic guests binding to lanthanide complexes *via* aromatic, non-covalent interactions. The tweezer shape of the complexes is tailored for the formation of a binding pocket. Europium shows the highest sensitisation with characteristic red luminescence for detection of aromatic guests which are common pollutants in aquatic environments.

The detection of aromatic pollutants in water is increasingly important following their widespread industrial use, especially in the cosmetic, dye and petrochemical industries, which leads to their presence in waste waters at elevated concentration affecting marine and plant environments.[1,2] Detection techniques rely mainly on chromatographic methods, which take considerable time for sample preparation and data processing and bear high costs requiring experienced personnel.[3] Optical methods are attractive for integration to portable platforms or fluidic devices to allow rapid, online monitoring, providing a suitable alternative.[4,5] Lanthanide luminescent probes have distinct advantages in optical sensing with characteristic line-shaped emission which is easily distinguishable from any background autofluorescence, high photostability and a palette of colours to choose based on the lanthanide choice for a specific ligand set.[6] Their luminescence signal has been used in multimetallic metal organic frameworks for detection of pollutants.[7–9] The design of water-soluble lanthanide receptors which are selective for aromatic compounds and yet provide a sensitive response in water remains a challenge. A paradigm platform was developed by Nocera *et al.*[10–12] which operates in aqueous systems and can be integrated in microfluidic devices. The hydrophobic cavity of cyclodextrins allows inclusion of a neutral aromatic guest, and the lanthanide emission is turned on by the formation of the assembly based on the cyclodextrin cavity. An alternative approach in receptor design for sensing is based on aromatic interactions as demonstrated in organic molecular tweezers where two aromatic groups are connected by a rigid linker.[13–15] The flexibility of the receptor cavities to allow for the best fit of the guest is important to maximise the interactions.[16–18] Zimmerman *et al.* have shown that a well-defined receptor allows stereochemical control of the guest binding with a 7 Å cavity between the aromatic groups.[15] Receptor designs relying on aromatic interactions for guest interaction and lanthanide luminescence sensitisation are attractive as there is no requirement of the guest/analyte to bind to the lanthanide. We wish to report herein responsive lanthanide tweezer-shaped complexes with hydrophobic arms for aromatic recognition sites. Our molecular receptor design is based on lanthanide complexes with DTPA-bisamide derivatives which are water soluble and provide a rigid framework around the lanthanide, while the lanthanide core is neutral, preventing other interactions.[19] They are popular ligands for Gd(III) and other lanthanides in application as MRI agents and radiopharmaceuticals.[20–25] We have been interested in their sensing properties using the available lanthanide coordination site to bind to analytes, replacing the coordinated water molecule.[26] Moreover, modifications on the DTPA-bisamide rigid framework position the lanthanide in directed multimetallic self-assemblies forming heterometallic Ln–Pt_2 hairpins for DNA binding,[27–29] Ln–Ln′ macrocyclic structures[30–32] and bi-functional attachment to gold nanoparticles.[33–36]

Herein, we investigate the sensitisation of lanthanide luminescence by aromatic guests based on the tailoring of the DTPA-bisamide arms for their binding (Scheme 1). We report the properties of the Eu(III) complexes of derivatives of DTPA bisamides, Eu**L**^{1} Eu**L**^{2}, Eu**L**^{3}, Eu**L**^{4} (Schemes 1 and 2) for aromatic pollutant binding based on the variation of the bisamide arms. Comparison with Tb(III) complexes is used to further understand binding properties and to assess strongest luminescence output. In the first two complexes, Eu**L**^{1} and Eu**L**^{2}, the amide arms differ only by a methylene unit, changing the flexibility of the amide, while the other two complexes Eu**L**^{3}, Eu**L**^{4} are compared for assessment of binding with no presence of a cavity or with a functional group to participate in CH–π or π–π aromatic interactions.

[a] School of Chemistry, University of Birmingham, Edgbaston, B15 2TT, UK. E-mail: z.pikramenou@bham.ac.uk
[b] School of Chemistry, Cardiff University, Cardiff, CF10 3AT, UK

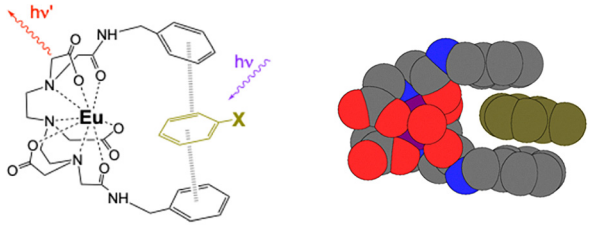

Scheme 1 Illustration of the Eu$\mathbf{L^1}$ pocket and MM2 model of Eu$\mathbf{L^1}$ with toluene guest based on Eu$\mathbf{L^1}$ X-Ray crystal structure.

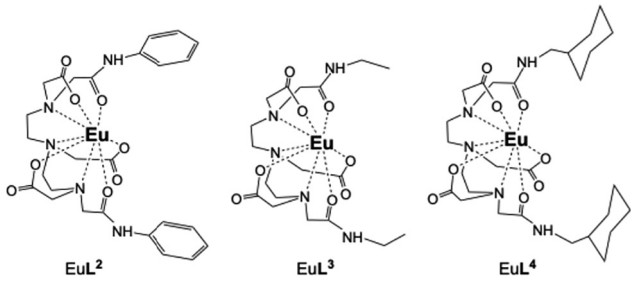

Scheme 2 Structures of Eu$\mathbf{L^2}$, Eu$\mathbf{L^3}$ and Eu$\mathbf{L^4}$.

The X-ray single crystal structure analysis of the two phenyl-derivatives, Eu$\mathbf{L^1}$ and Eu$\mathbf{L^2}$ confirms the presence of a pocket in Eu$\mathbf{L^1}$ (Fig. 1). There is an edge-to-face CH-π interaction of the two aromatic rings with a CH–C distance of 3.2 Å. The angle between the planes of the rings is 75.6° with a ring centroid-to-centroid distance of 5.7 Å. This pocket is not evident in Eu$\mathbf{L^2}$ where the phenyl arms are located further apart since the amide and the phenyl groups are coplanar due to conjugation. The ring centroid-to-centroid distance is ca 7.6 Å in this case and the angle between the ring planes is in the 41–54° range. There are two unique complex units in the crystal structure of Eu$\mathbf{L^2}$. In both cases the geometry around Eu(III) centre is a distorted capped square anti-prism with one coordinated water molecule as the capping group. A crystal structure of Y$\mathbf{L^2}$ shows comparable geometry to Eu$\mathbf{L^2}$.[23]

A comparison of the Eu–O and Eu–N bond lengths between Eu$\mathbf{L^1}$ and Eu$\mathbf{L^2}$ indicate the water molecule is less closely bonded in Eu$\mathbf{L^2}$ while the oxygen donors provide a tighter coordination around the Eu in $\mathbf{L^2}$.

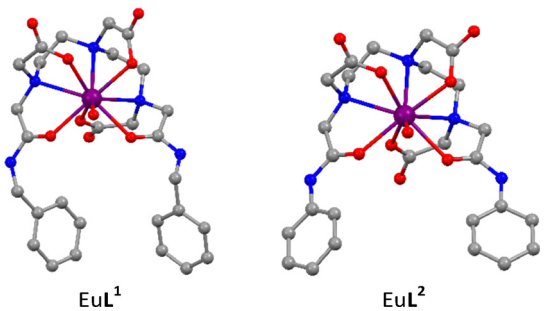

Fig. 1 The structures of Eu$\mathbf{L^1}$ (left) and Eu$\mathbf{L^2}$ (right) from X-ray single crystal diffraction. Oxygen and nitrogen atoms are represented as red and blue spheres, respectively. Hydrogen atoms have been omitted for clarity.

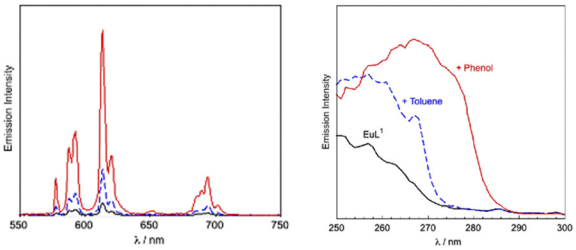

Fig. 2 Emission spectra (left) and excitation spectra (right) of Eu$\mathbf{L^1}$ (4×10^{-5} mol dm^{-3}) in water (black solid line), Eu$\mathbf{L^1}$ + excess toluene (blue dashed line, 40 equiv) and Eu$\mathbf{L^1}$ + 10 eq phenol (red line). λ_{exc} = 270 nm, λ_{em} = 613 nm.

Both Eu$\mathbf{L^1}$ and Eu$\mathbf{L^2}$ show luminescence characteristic of the europium signal with lifetimes of 0.55 ms and 0.51 ms in water respectively which increase to 2.5 and 2.2 ms in D_2O, revealing coordination of one water molecule to the Eu(III) centre in agreement with the crystal structure (SI). Addition of an excess of toluene or phenol to an aqueous solution of Eu$\mathbf{L^1}$ leads to a high Eu(III) luminescence signal enhancement in comparison to the very weak signal of Eu$\mathbf{L^1}$ (Fig. 2). Excitation spectra of these host–guest assemblies reveal characteristic absorption profiles of toluene and phenol, with peaks at 261 and 270 nm respectively, demonstrating that the signal enhancement is due to energy transfer to the Eu(III) centre from toluene or phenol. This could only occur if the guests were being brought into close proximity of the Eu(III) centre, as bimolecular energy transfer is not taking place at the low concentration conditions of the experiment. No luminescence enhancement is observed if the experiment is carried out in ethanol, which indicates the requirement of the aqueous environment to enhance the association of the guest. The luminescence lifetime of Eu$\mathbf{L^1}$ did not change upon addition of the guests.

To assess further the presence of the hydrophobic pocket, we studied the binding of phenol to three complexes with varied properties of the DTPA-bisamide arms: Eu$\mathbf{L^2}$ which has an open rigid arrangement of the phenyl arms, Eu$\mathbf{L^3}$ and Eu$\mathbf{L^4}$. In all three cases the addition of phenol under the same conditions presented no enhancement of the Eu(III) luminescence. For Eu$\mathbf{L^1}$, the observed enhancement is attributed to the methylene link of the phenyl moieties to the bisamide arms, which confers enough flexibility to optimise the pocket for interaction with the aromatic guests. The lack of any enhancement for Eu$\mathbf{L^4}$, which bears hydrophobic arms, indicates the requirement of the aromatic interactions in the guest binding.

To evaluate the strength of binding we have performed titration experiments of phenol and methoxybenzene guests. Titration of the guests into Eu$\mathbf{L^1}$ provided increase of the Eu(III) luminescence signal which reaches a plateau, fitting to binding constants of K = 3980 ± 100 and 3100 ± 100 M^{-1} for phenol and methoxybenzene respectively (Fig. 3).

To compare the relative Eu(III) signal enhancement of different guests we added the guests to reach isoabsorptive conditions and compared I–I_0/I_0 integrated signals. Phenol demonstrated the highest 10-fold enhancement followed by methoxybenzene 6-fold enhancement and 1,3 dimethoxybenzene with 1.5 fold

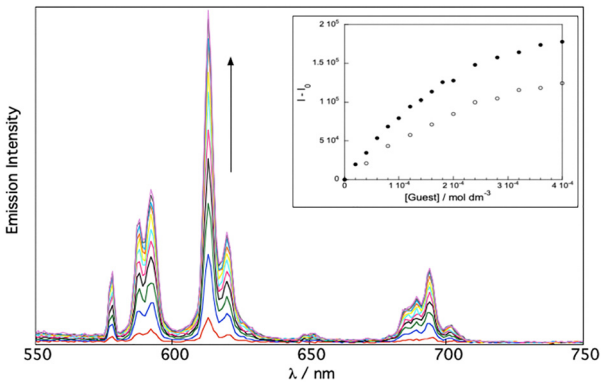

Fig. 3 Emission titration of phenol into Eu$\mathbf{L^1}$ (4×10^{-5} mol dm^{-3}), each spectrum corresponding to one equivalent addition of phenol (H_2O, 1% CH_3OH) λ_{exc} = 270 nm. Inset: binding curves showing change in integrated emission signal (I-I_o) upon addition of phenol (closed circles) and methoxybenzene (open circles).

enhancement. It is important to note that only 1.4 equivalents were used for 1,3 dimethoxybenzene. Other guests were tested to investigate maximum enhancement of signal; fluorobenzene only reached up to 2-fold enhancement whereas hexafluorobenzene, nitrobenzene and benzaldehyde did not lead to any enhancement. Fluorobenzene also provided a handle for monitoring the binding by ^{19}F NMR spectroscopy. Upon addition of 10 equivalents of Y$\mathbf{L^1}$ host complex into a solution of fluorobenzene in D_2O, the ^{19}F resonance shifted by −0.52 ppm from −113.05 ppm to −113.57 ppm (Fig. 4).^{19}F chemical shifts are sensitive to the environment and the observed shift is characteristic of the fluorine being in a more shielding environment within the aromatic pocket. The analogous Tb$\mathbf{L^1}$ complex was also tested as sensor. However, the relative enhancements are very small (only 2-fold for phenol) compared with the ones observed for Eu$\mathbf{L^1}$, even though the binding constant is in the same order of magnitude. This is attributed to the high background signal of Tb$\mathbf{L^1}$ as compared with Eu$\mathbf{L^1}$ which is not ideal for a turning-on sensor based on signal enhancement. There are several factors which contribute to the lanthanide signal enhancement. The low background signal of the lanthanide

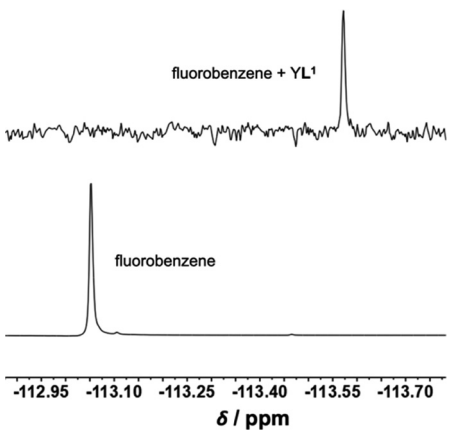

Fig. 4 ^{19}F NMR spectra of fluorobenzene upon addition of 10 equiv. of host Y$\mathbf{L^1}$ in D_2O (external reference CF_3COOH).

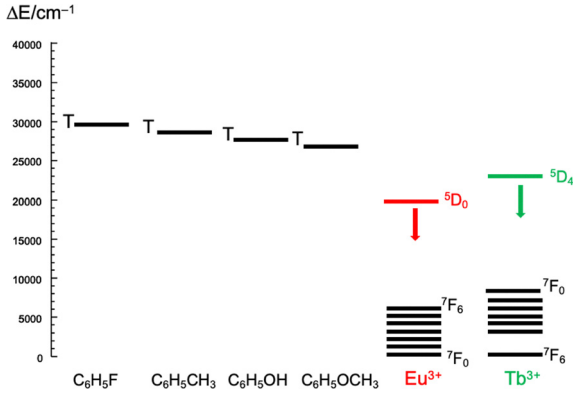

Fig. 5 Schematic energy diagram showing the triplet state energy levels of the guests and the lanthanide excited states.

tweezer complex is important for the sensitisation as it is known that the LMCT band from carboxylates in Eu(III) complexes decreases the Eu(III) luminescence. The amount of the tweezer-guest complex influences the output signal, and it is important to consider the guest size and the relevant guest dipole moment for the association with the host. Recent studies of the effect of substituents in the aromatic system[37] show the actual polarity of the group may be more important rather than the influence of the phenyl ring. Finally, the energy transfer efficiency depends on the gap of the sensitiser triplet state (Fig. 5). There seems to be very little difference between the energy states of the triplet states which are better suited for Tb(III). In our case, the highest signal observed results from an interplay between the polarity of the functional group and the slightly lower triplet state of the phenol/methoxy derivatives.

In summary, red luminescence from Eu(III) is triggered by binding of aromatic guests to a water-soluble Eu(III) complex. The arrangement of the amide arms in DTPA-bisamides is tailored for aromatic recognition to form a tweezer complex. The flexibility and size of the cavity is important in the binding to exclude any interaction of the aromatic pollutants outside the cavity, and the single linker of the methylene group provides flexibility for the formation of the complex. The work demonstrates that tuning of the luminescence properties of complexes through ligand and lanthanide selection can provide improved performance, such as Eu(III) providing optimal performance in this case over Tb(III). The maximum enhancement is observed for phenol and methoxybenzene, showing the potential for development of functional lanthanide complexes with variation of recognition groups in the arms of the DTPA-bisamide to introduce further selectivity in binding as well as tailoring the optical response. The luminescence response for aromatic pollutant binding is applicable in an-online detection platform where operation of aqueous samples is a requirement. Furthermore, these sensors have the potential to be modified for surface attachment to form a portable device for luminescence detection.

Investigation, methodology, analysis: P. G. Glover, L. Senkiw-Smith, L. Ruston, B. M. Kariuki. Writing original draft: P. B. Glover. Conceptualisation: P. B. Glover, L. Ruston, Z. Pikramenou. Writing: all authors. Supervision: Z. Pikramenou.

Conflicts of interest

There are no conflicts to declare.

Data availability

The supporting data have been provided as part of the supplementary information (SI). Supplementary information: Ligand and lanthanide complex synthetic procedures and characterisation; additional titration data; summary of crystal structure data. See DOI: https://doi.org/10.1039/d6cc00925e.

CCDC 1031054 and 1031055 contain the supplementary crystallographic data for this paper.[38a,b]

Acknowledgements

We wish to thank the University of Birmingham for support.

References

1 H. Mehta, P. Patel, A. Mukherjee and N. S. Munshi, *Clean:Soil, Air, Water*, 2023, **51**, 2100439.
2 C. Muangchinda, A. Rungsihiranrut, P. Prombutara, S. Soonglerdsongpha and O. Pinyakong, *J. Hazard. Mater.*, 2018, **357**, 119–127.
3 P. Gątarek, A. Rosiak and J. Kałużna-Czaplińska, *Crit. Rev. Anal. Chem.*, 2025, **55**, 840–857.
4 D. Li, H. Zhou, Z. Ren and C. Lee, *Small Sci.*, 2025, **5**, 2400250.
5 J. P. Anzenbacher, P. Lubal, P. Buček, M. A. Palacios and M. E. Kozelkova, *Chem. Soc. Rev.*, 2010, **39**, 3954–3979.
6 C. Alexander, Z. Guo, P. B. Glover, S. Faulkner and Z. Pikramenou, *Chem. Rev.*, 2025, **125**, 2269–2370.
7 X. Lian and B. Yan, *RSC Adv.*, 2016, **6**, 11570–11576.
8 S. Mukherjee, S. Dutta, Y. D. More, S. Fajal and S. K. Ghosh, *Dalton Trans.*, 2021, **50**, 17832–17850.
9 H. Zhang, D. Chen, H. Ma and P. Cheng, *Chem. – Eur. J.*, 2015, **21**, 15854–15859.
10 Z. Pikramenou and D. G. Nocera, *Inorg. Chem.*, 1992, **31**, 532–536.
11 Z. Pikramenou, J.-a Yu, R. B. Lessard, A. Ponce, P. A. Wong and D. G. Nocera, *Coord. Chem. Rev.*, 1994, **132**, 181–194.
12 C. M. Rudzinski, A. M. Young and D. G. Nocera, *J. Am. Chem. Soc.*, 2002, **124**, 1723–1727.
13 F.-G. Klärner and B. Kahlert, *Acc. Chem. Res.*, 2003, **36**, 919–932.
14 A. J. Goshe, I. M. Steele, C. Ceccarelli, A. L. Rheingold and B. Bosnich, *Proc. Natl. Acad. Sci. U. S. A.*, 2002, **99**, 4823–4829.
15 S. C. Zimmerman, C. M. VanZyl and G. S. Hamilton, *J. Am. Chem. Soc.*, 1989, **111**, 1373–1381.
16 M. Hardouin–Lerouge, P. Hudhomme and M. Sallé, *Chem. Soc. Rev.*, 2011, **40**, 30–43.
17 H. M. Colquhoun, Z. Zhu, C. J. Cardin, Y. Gan and M. G. B. Drew, *J. Am. Chem. Soc.*, 2007, **129**, 16163–16174.
18 M. Harmata, *Acc. Chem. Res.*, 2004, **37**, 862–873.
19 M. S. Konings, W. C. Dow, D. B. Love, K. N. Raymond, S. C. Quay and S. M. Rocklage, *Inorg. Chem.*, 1990, **29**, 1488–1491.
20 J. Ru, W. Xu, M. Kou, H. Dong, X. Tang, Y. Chen, L. Kang, L. Dai and C. Liang, *J. Mater. Chem. B*, 2023, **11**, 7182–7189.
21 J. Greiser, T. Hagemann, T. Niksch, P. Traber, S. Kupfer, S. Gräfe, H. Görls, W. Weigand and M. Freesmeyer, *Eur. J. Inorg. Chem.*, 2015, 4125–4137.
22 E. Debroye, S. V. Eliseeva, S. Laurent, L. Vander Elst, S. Petoud, R. N. Muller and T. N. Parac-Vogt, *Eur. J. Inorg. Chem.*, 2013, 2629–2639.
23 D. Parker, K. Pulukkody, F. C. Smith, A. Batsanov and J. A. K. Howard, *J. Chem. Soc., Dalton Trans.*, 1994, 689–693.
24 S. Vallabhajosula, *Molecular Imaging and Targeted Therapy*, Springer, 2023.
25 B. Achour, J. Costa, R. Delgado, E. Garrigues, C. F. G. C. Geraldes, N. Korber, F. Nepveu and M. I. Prata, *Inorg. Chem.*, 1998, **37**, 2729–2740.
26 L. L. Ruston, G. M. Robertson and Z. Pikramenou, *Chem. – Asian J.*, 2010, **5**, 571–580.
27 D. J. Lewis, P. B. Glover, M. C. Solomons and Z. Pikramenou, *J. Am. Chem. Soc.*, 2011, **133**, 1033–1043.
28 D. J. Lewis, F. Moretta and Z. Pikramenou, *Supramol. Chem.*, 2012, **24**, 135–142.
29 M. M. Castaño-Briones, A. P. Bassett, L. L. Meason, P. R. Ashton and Z. Pikramenou, *Chem. Commun.*, 2004, 2832–2833.
30 P. B. Glover, P. R. Ashton, L. J. Childs, A. Rodger, M. Kercher, R. M. Williams, L. De Cola and Z. Pikramenou, *J. Am. Chem. Soc.*, 2003, **125**, 9918–9919.
31 L. Scarpantonio, S. A. Cotton, E. Del Giorgio, M. McCallum, M. J. Hannon and Z. Pikramenou, *J. Inorg. Biochem.*, 2020, **209**, 111119.
32 D. J. Lewis, F. Moretta, A. T. Holloway and Z. Pikramenou, *Dalton Trans.*, 2012, **41**, 13138–13146.
33 A. Davies, D. J. Lewis, S. P. Watson, S. G. Thomas and Z. Pikramenou, *Proc. Natl. Acad. Sci. U. S. A.*, 2012, **109**, 1862–1867.
34 D. J. Lewis, C. Bruce, S. Bohic, P. Cloetens, S. P. Hammond, D. Arbon, S. Blair-Reid, Z. Pikramenou and B. Kysela, *Nanomedicine*, 2010, **5**, 1547–1557.
35 D. J. Lewis, T. M. Day, J. V. MacPherson and Z. Pikramenou, *Chem. Commun.*, 2006, 1433–1435.
36 A. C. Savage and Z. Pikramenou, *Chem. Commun.*, 2011, **47**, 6431–6433.
37 S. E. Wheeler and K. N. Houk, *J. Chem. Theory Comput.*, 2009, **5**, 2301–2312.
38 (*a*) CCDC 1031054: experimental crystal structure determination, 2026, DOI: 10.5517/ccdc.csd.cc13lwtd; (*b*) CCDC 1031055: experimental crystal structure determination, 2026, DOI: 10.5517/ccdc.csd.cc13lwvf.

